Atmos. Chem. Phys., 15, 8051–8064, 2015
www.atmos-chem-phys.net/15/8051/2015/
doi:10.5194/acp-15-8051-2015

Atmospheric Chemistry and Physics
Open Access

Increasing Arabian dust activity and the Indian summer monsoon

F. Solmon[1], **V. S. Nair**[2], **and M. Mallet**[3]

[1]The Abdus Salam International Center for Theoretical Physics, Strada Costiera 11, 34100 Trieste, Italy
[2]Space Physics Laboratory Vikram Sarabhai Space Centre Thiruvananthapuram Kerala, 695 022, India
[3]Laboratoire d'Aerologie CNRS, Université Paul Sabatier, 14 Ave, Edouard Belin, 31400 Toulouse, France

Correspondence to: F. Solmon (fsolmon@ictp.it)

Received: 6 January 2015 – Published in Atmos. Chem. Phys. Discuss.: 20 February 2015
Revised: 15 June 2015 – Accepted: 24 June 2015 – Published: 22 July 2015

Abstract. Over the past decade, aerosol optical depth (AOD) observations based on satellite and ground measurements have shown a significant increase over Arabia and the Arabian Sea, attributed to an intensification of regional dust activity. Recent studies have also suggested that west Asian dust forcing could induce a positive response of Indian monsoon precipitations on a weekly timescale. Using observations and a regional climate model including interactive slab-ocean and dust aerosol schemes, the present study investigates possible climatic links between the increasing June–July–August–September (JJAS) Arabian dust activity and precipitation trends over southern India during the 2000–2009 decade. Meteorological reanalysis and AOD observations suggest that the observed decadal increase of dust activity and a simultaneous intensification of summer precipitation trend over southern India are both linked to a deepening of JJAS surface pressure conditions over the Arabian Sea. In the first part of the study, we analyze the mean climate response to dust radiative forcing over the domain, discussing notably the relative role of Arabian vs. Indo-Pakistani dust regions. In the second part of the study, we show that the model skills in reproducing regional dynamical patterns and southern Indian precipitation trends are significantly improved only when an increasing dust emission trend is imposed on the basis of observations. We conclude that although interannual climate variability might primarily determine the observed regional pattern of increasing dust activity and precipitation during the 2000–2009 decade, the associated dust radiative forcing might in return induce a critical dynamical feedback contributing to enhancing regional moisture convergence and JJAS precipitations over southern India.

1 Introduction

Indian summer monsoon rainfall determines to a large extent food production for subcontinental India and has major socioeconomic impacts. Simulating monsoon precipitations variability from intra-seasonal to interannual timescales is identified as major challenge, especially in the context of climate change and increasing anthropogenic pressures over the Indian subcontinent. The complexity of the monsoon system arises from the interactions between physical processes involving atmosphere, land and ocean and operating over a wide range of spatial and temporal scales (Turner and Annamalai, 2012). The role of aerosol as a possible factor modifying these interactions, with consequences on precipitation variability, has been a subject of intense study for the last decade (Lau et al., 2008).

There are basically two mechanisms invoked when discussing the climatic response to direct aerosol forcing over southern Asia. The "solar dimming effect" (Ramanathan et al., 2005) proposes that the reduction in surface solar radiation due to absorption and scattering by aerosols, which shows a regional maximum over northern India and Indian ocean, induces a reduction of the north–south surface temperature gradients resulting in a weakening of the Indian summer monsoon. Consistently with this mechanism, the observed summertime drying trend observed over the central Indian region since 1950 has been attributed to increased anthropogenic aerosol emissions through a slowdown of the tropical meridional circulation (Bollasina et al., 2011). In contrast the "elevated heat pump effect" (Lau et al., 2006) proposes that radiative heating anomalies due to anthropogenic black carbon and dust transported over the Himalayan foothill and Tibetan plateau during the dry and pre-

monsoon seasons enhance meridional tropospheric temperature gradients, resulting in a strengthening and earlier onset of the Indian monsoon rainfall. The elevated heat pump effect has, however, been questioned by Nigam and Bollasina (2010). Though apparently antagonistic, both these mechanisms might be effective at different stages of the premonsoon and monsoon development (Meehl et al., 2008), indicating the complexity of aerosol climate feedbacks operating on different timescales. In addition it has been outlined that the regional impact of Asian aerosol might be reinforced by non-Asian sources through long distance transport and global dynamical adjustments (Bollasina et al., 2013; Ganguly et al., 2012; Cowan and Cai, 2011; Wang et al., 2009).

Despite a large focus on anthropogenic aerosol effects justified by the observed intensification of emissions contributing to the "Asian brown cloud" (Ramanathan et al., 2005), the potential importance of natural, and in particular dust, aerosol has been also recently highlighted (Jin et al., 2014; Vinoj et al., 2014): tt is suggested that west Asian dust outbreaks can induce a fast and regional atmospheric response which could explain observed positive correlation between aerosol optical depth (AOD) over west Asia and summer precipitation over India on a weekly timescale. Using global circulation model (GCM) experiments with prescribed sea surface temperature (SST), Vinoj et al. (2014) attributes the cause of this correlation to the large radiative heating induced by dust radiation absorption over Arabia and the Arabian Sea resulting in an intensification of southwesterly moisture convergence towards India. This mechanism involves primarily direct and semi-direct aerosol effects and is based on a fast reaction of monsoonal weather systems to dust radiative heating perturbation.

The question of characterizing the impact of west Asian dust on the Indian monsoon becomes even more relevant when we consider another striking fact: the observed recent enhancement of Arabian dust activity as measured by satellite and ground-based AOD observations during the past decade. Based on Sea-viewing Wide Field of View Sensor (SeaWIFS) satellite observations, a significant June–July–August increasing AOD linear trend has been determined for the period 1998–2010 for the Arabian region (Hsu et al., 2012). This regional trend, associated with a regional increase of dust storm activity, is also detected in ground-based photometer measurements from the Aerosol Robotic Measurement Network (AERONET) at the Solar village site in Saudi Arabia (Xia, 2011). To our knowledge, the attribution of this regional emission increase to climatic factors and/or land use change is yet to be fully investigated. Ginoux et al. (2012) discuss the possible increasing contribution anthropogenic dust sources relevant to the region, and we also indicate later some possible connections with the evolution of low-pressure conditions over the Arabian Sea and the Indian monsoon system.

In this context, the questions we wish to primarily address here are as follows: what are the main characteristic of dust radiative forcing regional climatic feedbacks, and to what extent could the recent enhancement of dust activity in the Arabian region affect the Indian monsoon dynamics and precipitations on a decadal timescale? As dust emissions might evolve naturally or/and as a result of climate and land use change (Mahowald, 2007; Mulitza et al., 2010; Yoshioka et al., 2007), characterizing and quantifying the regional climate implications of observed dust variability is especially relevant for a better understanding of the Indian monsoon system variability and its possible evolution.

Toward this goal, we use a 50 km resolution regional climate model coupled to an aerosol scheme and a slab-ocean model together with diverse observation and reanalysis products. Specific attention is paid to the quality of the simulated Indian monsoon circulation and precipitation fields as well as to the representation of aerosols notably in term of sources, optical depth, radiative forcing and heating rates gradients. In our approach, we believe that the simulation domain size is large enough to capture important regional dynamical feedbacks to the aerosol radiative perturbation. As a caveat we acknowledge that large-scale dynamical feedbacks arising from the possible aerosol-induced excitation of planetary waves (Rodwell and Jung, 2008) cannot be accounted for using a limited area model. Knowing in what proportion the effective regional climatic response to aerosol forcing is dominated by regional vs. global dynamical adjustments is, however, a matter of debate (Ramanathan et al., 2005; Bollasina et al., 2011; Ganguly et al., 2012; Cowan et al., 2011). In Sect. 1 we detail the modeling experiments as well as the different data sets and methods used for trend calculation. Section 2 focuses on analyzing observed summer AOD and precipitation trends and interannual correlations over the domain. Dust radiative and climatic impacts and the possible links between Arabian dust trend and southern India precipitation at the decadal scale are then addressed in Sects. 3 and 4.

2 Data and methods

2.1 Regional climate model

We use the International Center for Theoretical Physics regional climate model RegCM4 (Giorgi et al., 2012) at 50 km resolution. Runs are performed on the COordinated Regional climate Downscaling Experiment (CORDEX)-India domain over the period 1999–2009 including a 1-year spin up. Boundary conditions are provided by ERA-Interim reanalyses through a 1000 km buffer zone. The Newtonian relaxation to large-scale fields applied in the boundary buffer zone is designed to limit wave reflections in the domain as much as possible (Marbaix et al., 2003). Important physical options we used for this study are the Community Land Model version 3.5 (CLM3.5) (Tawfik and Steiner, 2011), the University of Washington turbulence scheme (O'Brien et al.,

2012) and the Emanuel convection scheme (Emanuel, 1991) with enabled tracer transport capabilities. The RegCM4 aerosol scheme includes a representation of anthropogenic sulfates, black and organic carbon (Solmon et al., 2006; Qian et al., 2001) as well as sea-salt and dust aerosol. For anthropogenic emissions, we use the Regional Emission inventory in ASia (REAS) (Ohara et al., 2007; Nair et al., 2012) completed by the Atmospheric Chemistry and Climate Model Intercomparison Project (ACCMIP) emissions (Lamarque et al., 2010) to account for biomass burning emissions and REAS-uncovered regions. For natural particles, sea-salt aerosol emissions are calculated online and are represented by two (sub- and super-micronic) different bins (Zakey et al., 2008). The dust emission scheme (Marticorena and Bergametti, 1995; Zakey et al., 2006) includes updates of soil texture distribution following Menut et al. (2013) and emission size distribution (Kok, 2011; Nabat et al., 2012). Lateral boundary conditions for aerosols are prescribed from a decadal climatology obtained from global runs performed using CAM-Chem model (J. von Hardenberg, personal communication, 2014). Dusts are represented using four bins and impact short- and long-wave radiation transfer as detailed in the Supplement (Table S1). All other aerosols impact the RegCM shortwave radiation scheme through pre-calculated optical properties (Solmon et al., 2006). Only the first indirect effect is accounted for and applied to sulfate aerosol (Giorgi et al., 2003).

Of particular importance for studying aerosol effects (Miller et al., 2004; Zhao et al., 2011), we implemented in RegCM4 a "flux-corrected" slab-ocean parameterization following an approach used in the FMS model (http://www.gfdl.noaa.gov/fms-slab-ocean-model-technical-documentation). This parameterization assumes a 50 m depth ocean mixed layer for which we calculate a prognostic SST through a simple energy budget. The lack of ocean dynamics, diffusion and convection as well as other model surface flux errors are compensated by specifying surface flux adjustments (q flux adjustments) to the slab temperature tendency equation, notably in order to maintain a realistic SST seasonal cycle compared to observations. To derive the q flux terms, we perform first a "restoring run" (with no interactive dust aerosol) where the slab prognostic SST are restored to observations, taken here as the Optimum Interpolation Sea Surface Temperature (OISST) (Reynolds et al., 2002), and considering a 5-day restoring timescale. As the slab mixed layer model is integrated (over the 1999–2009 period in this experiment), the restoring heat fluxes (q flux) calculated through this procedure are archived and saved in a monthly mean climatology at the end of the restoring run. Once the q flux climatology is built, the control and experimental "adjusted runs" are performed accounting for q fluxes (prescribed from the climatology) in the slab-ocean temperature equation. Over the domain, seasonal average differences of SST between the q flux adjusted control experiment and OISST observations vary in the range of -1 to 1°, ensuring that prognostic SSTs in the adjusted runs do not diverge much from observations and follow a realistic seasonal cycle. This approach extends previous aerosol regional climate studies based on forced SST over the Indian monsoon and other domains (e.g., Das et al., 2014).

The control experiment consists of three ensemble members of adjusted runs with no interactive dust aerosol activated (*nodust*). An ensemble of three adjusted runs is then performed with activation of dust (*dust*). Additionally, a sensitivity test consisting of removing the Indo-Pakistani regional dust source (*dust_noIP*) is also performed. Finally an experiment of three ensemble members is done by imposing an increasing emission trend over Arabia in order to better reproduce observed AOD trends (*dust_ft*). This is done by increasing the saltation flux erodibility factor (Marticorena and Bergametti, 1995) during the run. From year 2004 to 2009 the corresponding increase of erodibility factor is about 30 %. In order to limit the effect of internal variability on our analysis of the aerosol feedbacks, we impose a small random perturbation in boundary conditions to every ensemble member during the run following O'Brien et al. (2011). With this technique, we increase the filtering of noise vs. statistically significant physical signal while performing differences between the ensemble means of perturbed and control run experiments. All results, figures and discussion are based on ensemble means.

2.2 Aerosol optical depth trend calculation

June–July–August–September (JJAS) AOD linear trend calculations are first performed using SeaWIFS monthly AOD (550 nm) products at 0.5° and regridded on the 50 km RegCM grid. Algorithms and validity of AOD retrievals from SeaWIFS atmospheric corrections are discussed in Sayer et al. (2012a, b). Moreover, as argued in Hsu et al. (2012), the SeaWIFS AOD product is recognized as a "stable" data set minimizing sensor calibration impact on trend analysis. For each model grid column, the SeaWIFS AODs are first deseasonalized applying a 13-term moving average for trend first guess and a stable seasonal filter for removing of the seasonal cycle (Brockwell and Davis, 2002). The deseasonalized times series of JJAS 2000–2009 are then extracted and a linear regression is applied on this subset to determine the JJAS linear trend. Statistical significance of the trend is determined using an F test and we plot only statistically significant pixels with a significant non-zero slope (p value < 0.05). Over our region of interest this treatment shows much consistency with the results of Hsu et al. (2012). The same method is applied to simulated monthly AOD time series for model–measurement comparison. Over the particular location of Solar Village, the deseasonalized JJAS AOD time series is also calculated from the Aerosol Robotic Network (AERONET) monthly optical depths and considering the average of AODs measured at 440 and 640 nm.

In addition to SeaWIF, we also make use of the Multiangle Imaging Spectro-Radiometer (MISR; Martonchik et al., 2004) retrievals for the validation of mean AOD and further interannual variability analysis.

2.3 Precipitation trend calculation

For the 2000–2009 precipitation trend calculation over southern India (Fig. 1b), we use the University of East Anglia Climate Research Unit product (CRU) (Harris et al., 2014), the Tropical Rainfall Measuring Mission (TRMM 3B42) (Huffman et al., 1995) product, the University of Delaware product (UDEL) (Matsuura and Willmott, 2009) and the Precipitation Estimation from Remotely Sensed Information using Artificial Neural Networks (PERSIANN) product (Ashouri et al., 2015). For each data set, monthly precipitation time series are first geographically averaged over a continental southern Indian box (5–20° N, 60–80° E). Deseasonalized time series are produced following a similar method than for AOD treatment. A yearly series of JJAS average precipitation is then produced by averaging the different deseasonalized series from each data sets and keeping the minimum and maximum values for estimation of the spread between different observation data sets.

Additionally, for the evaluation of simulated mean JJAS precipitation we also use the Asian Precipitation – Highly Resolved Observational Data Integration Towards Evaluation of water resources (APHRODITE) data set over the 2000–2007 period (Yatagai et al., 2012).

3 AOD vs. precipitation trends and interannual variability correlations

Linear trends of JJAS AODs, calculated from SeaWIFS observations over our domain (cf. Sect. 2), are presented in Figs. 1 and 3a. As already reported in Hsu et al. (2012), a significant positive trend is found over the Arabian Peninsula region. In addition, a positive AOD trend observed at the AERONET station of solar village (Xia, 2011) is also reported (Fig. 1a). As discussed in Hsu et al. (2012), a decreasing trend in AERONET-retrieved Ångstrom coefficients has been observed at Solar Village, indicating an enhanced contribution of larger particles to AODs over the decade. Together with the fact that AOD trends are due to an amplification of seasonal cycle coincident with dust seasonal maximum, this indicates that the Arabian region positive AOD trends are mainly due to increasing dust emission activity vs. a possible anthropogenic contribution. From the time series in Fig. 1a, we note that the JJAS observed deseasonalized AODs tends to steepen around year 2005. Consequently the 2005–2009 pentad shows sensibly higher averaged AODs relative to the 2000–2004 pentad. For simplifying the following discussion we will refer to these pentads as "NONDUSTY" and "DUSTY".

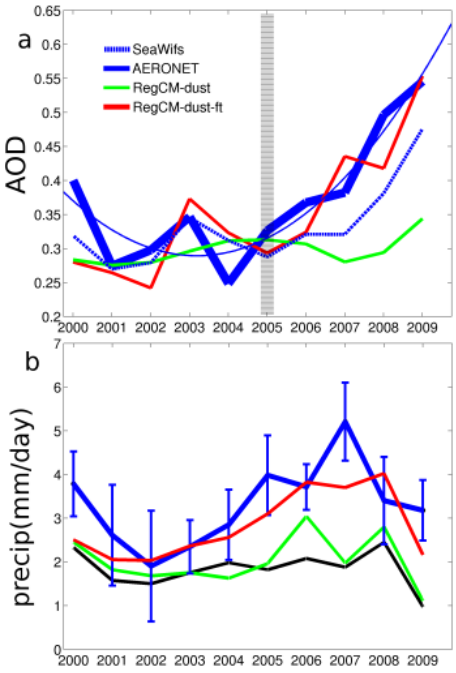

Figure 1. Arabian AODs and southern India deseasonalized precipitation trends during the decade 2000–2009. **(a)** The thick blue line represents monthly deseasonalized time series of JJAS AODs obtained from the Solar Village AERONET station (monthly product, average of 480–640 nm spectral bands). A quadratic regression fit, showing the progressive intensification of observed dust activity, is superimposed (blue curve). The blue hatched line represents the deseasonalized AOD time series obtained from SeaWIFS AOD interpolated on the Solar Village station. The green lines represent the monthly deseasonalized time series (as well as the corresponding quadratic fit) of JJAS AODs simulated by the model in *dust* simulation. The red lines represent the monthly deseasonalized time series (as well as the corresponding quadratic fit) of JJAS AODs simulated by the model with forced dust emission trends (*dust_ft* simulation). **(b)** The blue line represent the yearly time evolution of observed continental precipitation averaged for JJAS, over a southern India box (5–20° N, 60–80° E) and for different data sets (TRMM, CRU, PERSIANN). The blue bars materialize the amplitude between maximum and minimum values amongst observations for a given year. The equivalent deseasonalized JJAS average simulated precipitations are reported for the *nodust* simulations (black line), the *dust* standard simulations (green line) and the forced emission trend *dust_ft* simulations (red line). All modeling results represent a three-ensemble-member mean.

An increasing trend for precipitation over southern and eastern India is also detected in several data sets as illustrated in Fig. 1b. In a rather similar way to Arabian AODs, the observed JJAS precipitation in Fig. 1b shows a relative intensification for DUSTY relative to NONDUSTY pentads. If we plot the mean surface pressure and circulation differences between DUSTY and NONDUSTY pentads from ERAI and NCEP2 reanalyses (Figs. 4a and S3), we observe that both data sets show a cyclonic pattern over the eastern Arabian

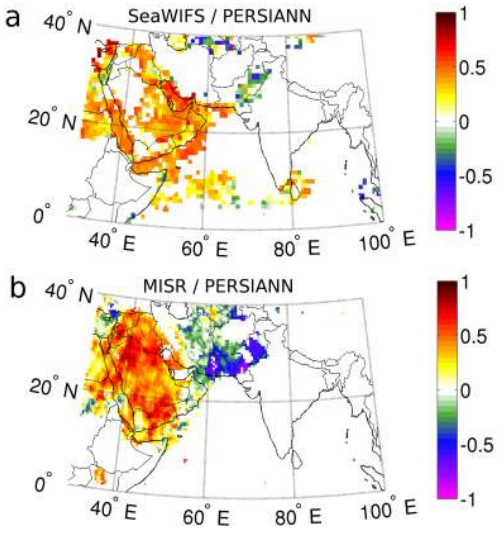

Figure 2. Interannual variability correlation coefficients calculated between deseasonalized summer (JJAS) AODs and deseasonalized JJAS precipitations averaged over a southern India box (5–20° N, 60–80° E): **(a)** based on the SeaWIFS AOD retrieval over the 1999–2010 period and **(b)** based on MISR AOD retrieval over the 2000–2010 period. Pixels showing monthly AOD < 0.2 are excluded from the calculation as well as pixels for which sampled valid year number is less than 8.

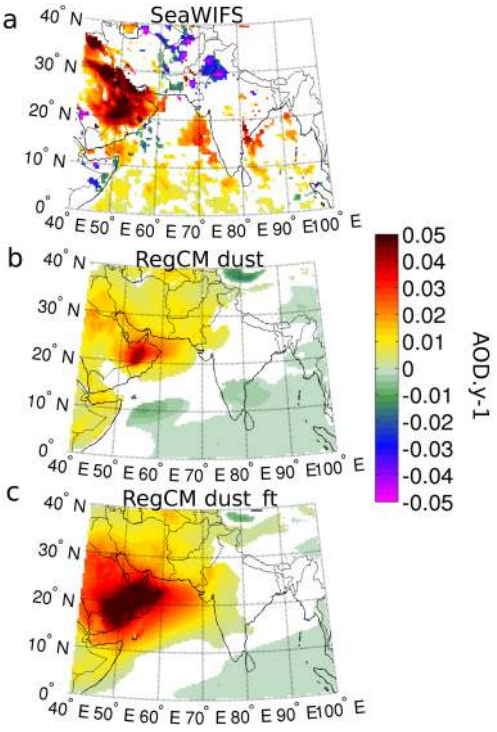

Figure 3. Linear JJAS AOD trend calculated over the 2000–2009 period from **(a)** SeaWIFS monthly observations, **(b)** model standard *dust* simulations and **(d)** model *dust_ft* simulations including a forced emission trend over the Arabian Peninsula. Only statistically significant trends (p value < 0.05) are represented (cf. Sect. 2). All modeling results represent a three-ensemble-member mean.

Sea and India with enhanced southwesterly circulation toward continental India. The associated increase of moisture flow over southern India is a likely reason for enhanced precipitation during DUSTY pentad relative to NONDUSTY pentad observed in precipitation data sets in Fig. 1b.

Furthermore, the cyclonic pattern found in pentad differences depicts a relative increase of the frequency/intensity of low-pressure situations over the northern Arabian Sea for DUSTY relative to NONDUSTY pentad. Such conditions are favorable to enhanced Shamal wind (Hamidi et al., 2013; Notaro et al., 2013) and could thus be a likely reason for the observed increase of AODs during the decade. On short timescales, it is also known that individual storms moving in the Arabian Sea and the northern Bay of Bengal can trigger large dust emission from Arabia and the Indo-Pakistani–Iran desert regions (Kaskaoutis et al., 2014; Ramaswamy, 2014). Based on these observations, both enhanced precipitation over India and Arabian dust AODs increase could be linked to lower pressure conditions prevailing over the Arabian Sea during DUSTY relative to NONDUSTY pentads. Reasons for these conditions are likely a feature of climate decadal variability over the region (Patra et al., 2005) and further analysis is beyond the scope of this study.

If the arguments developed above are valid, one should also expect a possible correlation between the interannual variability of summer dust AODs and precipitation over southern India. This correlation is not obvious in Fig. 1 for the case of Solar Village AODs. In order to get a more regional picture, we extend our analysis by calculating interannual correlations between observed deseasonalized summer AODs (based on SeaWIFS and MISR data) and deseasonalized summer precipitation over the previously defined southern India box (based on the PERSIANN data set). We consider the 1999–2010 period for SeaWIFS and 2000–2010 for MISR, excluding pixel with JJAS AOD < 0.2 in the process. Pixels with less than 8 years of valid JJAS observations over the period are excluded of the correlation calculation as well. Evident caution must be taken while interpreting the values of correlation coefficients due to the limited sample size. Nevertheless, in Fig. 2a and b our analysis reveals clear regional patterns: over the Indo-Pakistani source region both MISR and SeaWIFS deseasonalized summer AODs tend to be anti-correlated with southern Indian deseasonalized precipitations. Inversely, over Arabia, positive correlation coefficients tend to be observed for both MISR and SeaWIFS. This analysis has been repeated using the TRMM precipitation data set with no significantly different results (not shown here). Despite the fact that correlations are not very strong, the homogeneity of regional patterns and their consistency through different observational data sets lead us to think that a relation exists between the interannual variability

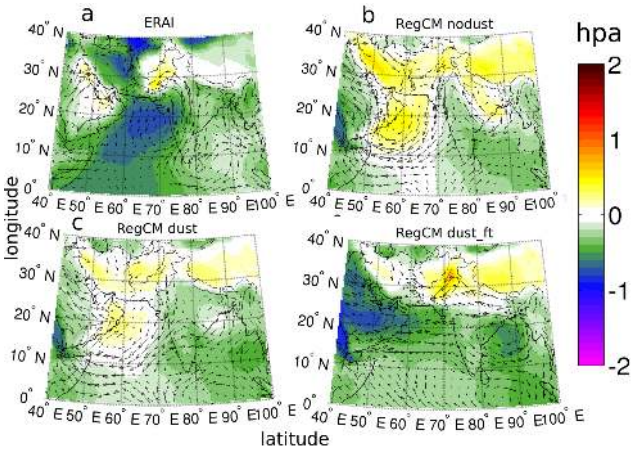

Figure 4. Difference of mean JJAS 850 hpa circulation and surface pressure between DUSTY (2005–2009) and NONDUSTY (2000–2004) pentads as defined in the text and calculated from **(a)** ERAI reanalysis, **(b)** "*nodust*" simulations, **(c)** "*dust*" standard simulations and **(d)** "*dust_ft*" simulations with forced emission trend over Arabia. As a complement to ERAI, an equivalent graph has been produced from NCEP reanalyses and displayed in Fig. S1 in the Supplement. All simulated results represent a three-ensemble-member mean.

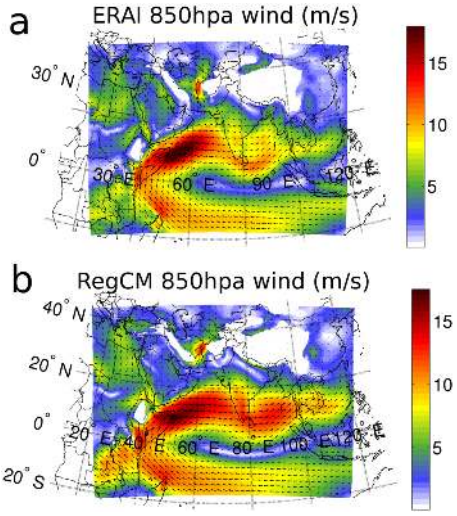

Figure 5. Mean 850 hpa JJAS wind intensity and direction as seen in **(a)** the ERAI reanalysis and **(b)** the RegCM *nodust* simulation for the period 2000–2009 and over the CORDEX-India domain. All modeling results represent a three-ensemble-member mean.

of dust sources activity and Indian precipitation. This relation is in line with the previous argument linking cyclonic activity in the Arabian Sea, associated with more summer precipitation over India and Pakistan, and enhanced Arabian dust emissions. Contrarily to the Arabian Peninsula, the Indo-Pakistani region is affected by Indian monsoon rainfall. The anti-correlation obtained over this region could thus possibly be explained by enhanced particle wet deposition and/or inhibiting effect of soil moisture on dust emissions during rainy years.

4 Simulation of dust radiative forcings, trends and associated feedbacks

4.1 Simulation of mean JJAS climate

In this section we assess the model capacity to simulate the mean observed JJAS monsoon circulation and precipitation over the domain. Comparison of simulated JJAS 850 hpa circulation patterns show an overall consistency with ERA-Interim reanalysis in terms of pattern and intensity as illustrated in Fig. 5a and b. The main differences are a moderate underestimation of easterly circulation in the region of the Somali Jet and a tendency for the model to overestimate average wind speed over the Bengal Gulf and Indonesia. Model mean JJAS precipitations are evaluated using TRMM, PERSIANN and the high resolution APHRODITE data sets (cf. Sect. 1). The variability between observations is illustrated in Fig. 6, c, e and g. As in many modeling studies and due to the complexity of convective and dynamics processes, important precipitation overestimation biases are found in regions of low precipitation as well as over the northeastern Himalayas and over the southern Bay of Bengal (Fig. 6). Over continental India, the control simulation (*nodust*) tends to produce drier conditions than observed, with a relative bias increasing toward eastern and southern India (Fig. 6d, f, h). The model shows better results when compared to the high-resolution APHRODITE rain-gauge-based data set (Fig. 6g–h). A comparison of Fig. 6b and 6d, f and h shows that radiative effects of dust tend to reduce model biases over southern and northwestern regions of continental India (see also Fig. S4). Biases are, however, increased over the western Bay of Bengal. Overall the simulated mean circulation and precipitation biases obtained in these simulations are either lower or comparable with CMIP5 state-of-the-art GCMs and multi-model ensemble (Sperber et al., 2013).

4.2 Simulation of aerosol optical depth, radiative forcings and heating rates

The climate response to aerosol via direct and semi-direct effects is strongly dependent on radiative forcing gradients as well as the vertical distribution of radiative heating due to aerosol. To evaluate model performance in this regard, the AOD simulated for both anthropogenic and natural aerosol is evaluated using MISR and SeaWIFS products described in Sect. 1 (Fig. 7). Simulated AODs in regions dominated by anthropogenic emissions (northeastern India, China, Indonesia) are reasonably captured despite local underestimations for Indian and Chinese megacities. An underestimation of simulated AODs over the Bay of Bengal is, however, noted, which

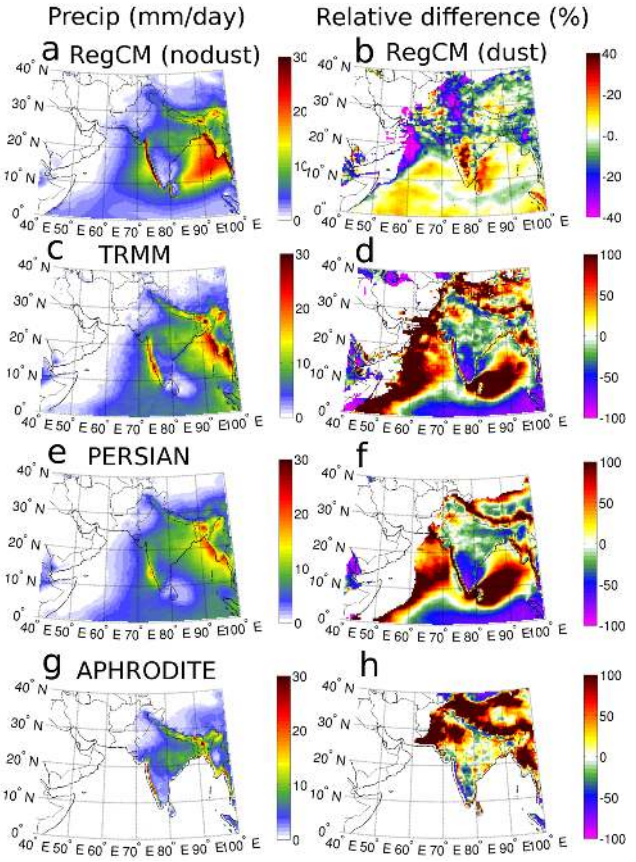

Figure 6. **(a)** Mean JJAS 2000–2009 precipitation simulated by the model in "*nodust*" configurations. **(b)** Relative difference in precipitation between *dust* and *nodust* simulations for JJAS 2000–2009 and calculated as $(dust - nodust\ /\ nodust) \times 100$. **(c)** JJAS 2000–2009 TRMM precipitation. **(d)** Relative difference (bias) between *nodust* and TRMM precipitations for observed precipitation level $> 0.2\,\mathrm{mm\,day^{-1}}$. **(e–f)** Same than **(c–d)** for the PERSIANN data set. **(g–h)** Same than **(c–d)** for the APHRODITE data sets but calculated for JJAS 2000–2007 only. All modeling results represent a three-ensemble-member mean.

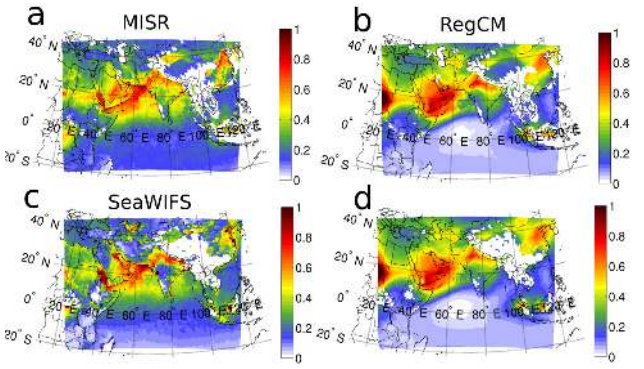

Figure 7. JJAS 2000–2009 AODs seen from the **(a)** MISR sensor and **(b)** as simulated by RegCM "*dust*" simulation for the full CORDEX-India domain. JJAS composite averages are built form monthly observations and model outputs. Regions of missing observations are screened out from the model averages. **(c, d)** Same as **(a, b)** but using the SeaWIFS AOD observations. All modeling results represent a 3 member's ensemble mean.

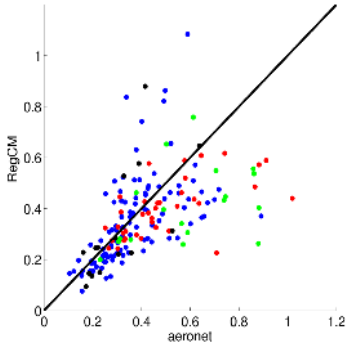

Figure 8. Simulated monthly AODs vs AERONET measured monthly AODs for the period of 2000–2009. Blue dots represent the solar Village Station (46.40° E, 24.90° N), red dot represent the Karachi station (67.03° E, 24.87° N), green dots represent Kuwait Airport station (47.98° E, 29.22° N) and black dots the Meizera station (53.8° E, 23.15° N). The correlation coefficient between data and measurements is equal to 0.59 and the root mean square error is 0.16.

can be due to uncertainties in emissions, notably for biomass burning (Streets et al., 2003), and/or an excessive deposition rate due overestimated precipitations as discussed previously. Overall, simulated JJAS 2000–2009 AODs show a very good agreement with observations both in term of magnitude and spatial gradients, providing additional regional details when compared to existing GCM simulations (e.g., Vinoj et al., 2014; Bollasina et al., 2011; Lau et al., 2006). Of particular importance, the dust-dominated regions of the Arabian Peninsula, the Arabian Sea and the Indo-Pakistani desert regions are quite accurately represented in terms of averaged JJAS AOD, although a likely small contribution of non-dust aerosol might play a part in this comparison.

Additional comparisons of simulated AODs and ground-based AERONET-retrieved AOD (500 nm) are proposed in Fig. 8 for the stations of Solar Village, Meizera, Kuwait Airport and Karachi. Dust aerosol mass is known to be dominant over these stations except perhaps during winter season over Karachi. For both model and observations, monthly averages are built from daily means and screened for missing days in observations. Figure 8 shows that the model tends in general to slightly underestimate observed AODs. This underestimation is perhaps more pronounced for the Karachi station, as also shown on JJAS average AOD comparisons (Fig. 7). The simulation of AOD seasonal cycles shows an overall consistency with observations (Fig. 9a, c). However, we note that for certain years AOD spring maxima tend to be underesti-

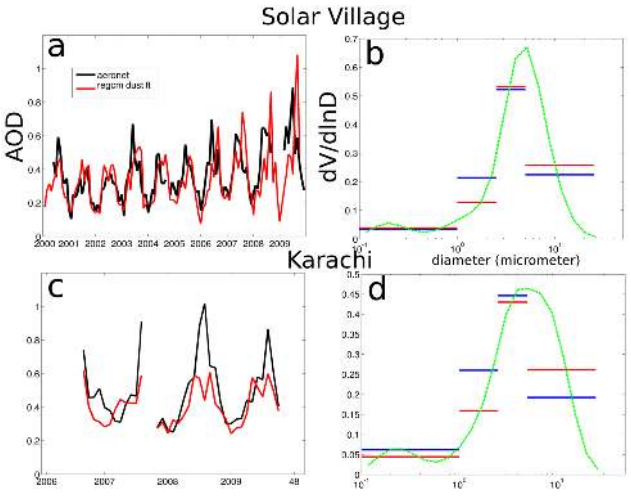

Figure 9. **(a)** Comparison between simulated and AERONET monthly AODs (see text) for Solar Village station. **(b)** Comparison of simulated and measured aerosol normalized volume size distribution averaged for JJAS 2009 over Solar Village. For comparison, the AERONET normalized volume distribution (green dotted line) is re-binned using a weighted average between model bins cutoff diameters (red lines). Blue lines show the corresponding simulated four-bin distribution for the same cutoff diameters. **(c)** Same as **(a)** for Karachi station. **(d)** Same as **(b)** for Karachi station.

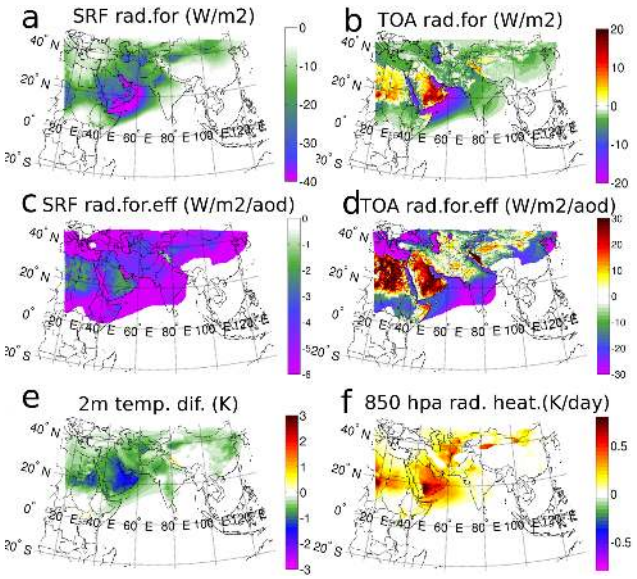

Figure 10. **(a)** JJAS 2000–2009 dust aerosol surface radiative forcing diagnostic. **(b)** JJAS 2000–2009 dust top-of-atmosphere radiative forcing diagnostic. **(c** and **d)** Corresponding surface radiative forcing efficiencies. **(e)** JJAS 2000–2009 2 m temperature difference between *dust* and *nodust* simulations. **(f)** 850 hpa radiative heating rate difference between *dust* and *nodust* simulations. All modeling results represent a three-ensemble-member mean.

mated by the model over solar village, while summer peaks tends to be overestimated. This slight shift of the seasonal cycle is also discussed in Shalaby et al. (2015).

In Fig. 9b and d we compare simulated aerosol size distribution to size distributions retrieved by AERONET inversions and re-binned to match model dust bins. Due a to lack of observational data and given the scope of the study, we restrict this comparison to JJAS 2009. Interannual variation of JJAS size distribution might anyway be of secondary order, especially given the possible uncertainties in AERONET inversions (Dubovik and King, 2000). For both Solar Village and Karachi, the model tends to show a consistent relative distribution between size bins compared to observations. However, we can note an overestimation of simulated fine and/or medium bins compared to underestimated coarse bins, especially in the case of Karachi (Fig. 9d). One of the possible reasons for this might lie in the emission size distribution (Kok, 2011), which tends to be more uncertain with regards to representing coarse particles, as for example discussed in Mahowald et al. (2014). Other reasons could be linked to accuracy of sources' geolocation, removal and transport processes. Bearing in mind observational uncertainties, the implication of a simulated dust size distribution shifted towards smaller particles would be to enhance shortwave scattering vs. absorption and long-wave emission with implications for radiative forcing and feedback discussed further. With possible compensating effects, note that dust refractive indices considered in this study are issued from the OPAC database (cf. Supplement), which could enhance absorption as noticed in Kaufman et al. (2001), Moulin et al. (2001) and Balkanski et al. (2007).

Over dust-dominated regions, the net dust surface radiative forcing (Fig. 10a) is dominated by shortwave cooling vs. positive long-wave surface warming as reported in the Supplement (Fig. S1). This induces a surface temperature cooling illustrated in Fig. 10e which can reach -2 K in subregions of Arabia. Over the ocean, a surface cooling is also obtained through the slab-ocean response but tends to be less effective due to larger surface thermal inertia. SST cooling reaches up to -1 °C close to Oman Gulf with a decreasing gradient towards India (Fig. 10e). As a result of both dust optical properties and surface albedo, top-of-atmosphere (TOA) radiative forcing is mostly positive over the high emission region of the Arabian Peninsula and become negative above the ocean and continental India. Note that in comparison to the Arabian Peninsula, the TOA radiative forcing efficiencies (i.e., TOA normalized by AOD reported in Fig. 10d) show less of a warming effect in the Indo-Pakistani desert regions due essentially to lower surface albedo. Over continental India the TOA radiative forcing efficiencies becomes largely negative due to relatively dark albedo and also due to the fact that long-range transported dust from Arabian and Indo-Pakistani sources are finer and more scattering. Uncertainties and regional variability in dust size distribution and optical properties might affect the magnitude and even the sign of the

radiative forcing simulated here with potential consequences for regional climate feedbacks, which are discussed further.

Atmospheric radiative heating rate anomalies primarily associated with dust radiative absorption are presented in Figs. 10f and S2. Mean simulated values for JJAS range from more than 1 K day^{-1} over source regions of Arabia to about 0.3 K day^{-1} in the core of the Arabian dust outflow, located between 850 and 600 hpa. Over India, the JJAS dust radiative warming at 850 hpa reaches about 0.05 to 0.1 K day^{-1}. These values are in the range of different observational studies (Moorthy et al., 2009; Kuhlmann and Quaas, 2010; Nair et al., 2008). We note that when radiative and moist processes feedbacks are combined, the diabatic heating induced by dust is, however, significantly lower than the 2 K day^{-1} warming reported in Vinoj et al. (2014), which can also explain differences further discussed in Sect. 4.3.

4.3 Mean monsoon response to dust radiative forcing

Regional climate adjustments to dust radiative forcing are first discussed by comparing "*dust*" and "*nodust*" simulations (as defined in Sect. 1) for JJAS 2000–2009. Figure 11a presents 850 hpa circulation and geopotential height (GPH) anomalies induced by dust direct and semi-direct effects over the domain. Two patterns emerge from this comparison: the first one is a low GPH anomaly centered over the southern Arabian Peninsula associated with a cyclonic circulation and the second one a positive GPH anomaly roughly centered over northeastern India associated with an anticyclonic anomaly. Regions of large positive or negative values in 850 hpa GPH difference patterns tend to match closely the regional TOA radiative forcing patterns (Fig. 10b). Over Arabia, dust radiative warming is maximum due to high concentrations of dust while dust surface cooling efficiency is relatively reduced due to high surface albedo. This induces a deepening of the Arabian thermal low (Fig. 11) and dry convection collocated with the maximum of dust radiative warming (Fig. S2c and d). On its southern part, the cyclonic circulation anomaly is associated with an intensification of the Somalia jet and eastward circulation between 10 and 20° N and 50 and 75° E. This intensification induces an enhanced convergence of moisture flux toward southern India and an increase of convective activity and precipitations over the southern Indian continent (Figs. 11 and S2d, e). From these simulations we estimate that this mechanism could enhance average precipitation by up to 10 % in southern India, thus contributing to the improvement of the model dry bias (Fig. 6a). Up to roughly 20° N, our results show much similarity with GCM results notably reported in Vinoj et al. (2014). One noticeable difference, however, is that while Vinoj et al. (2014) obtain an increase of precipitation over northern Arabian Sea, northwestern India and Pakistan, convective precipitations tend to be inhibited for these regions in our case. This regional stabilization is induced by a relatively large surface radiative dimming which decreases continental and sea surface temperatures (Fig. 10e) and predominate over dust diabatic warming effects. This is consistent with a negative simulated TOA radiative forcing (Fig. 10b). Such mechanisms have been analyzed in great detail by Miller et al. (2014). On average, in our simulations the combined contribution of Arabian and Indo-Pakistani dust sources appears to have a dual signature resulting in a strengthening of the Somali Jet, moisture convergence and precipitation over southern India while inhibiting convective precipitation and decreasing monsoon intensity north of about 20° N (Fig. 11).

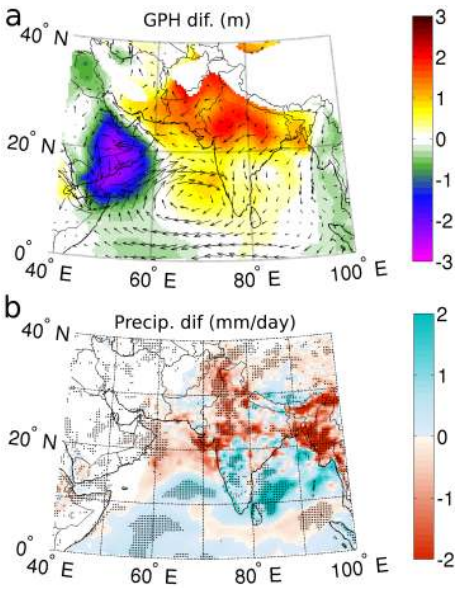

Figure 11. Dust impact on the mean monsoon dynamic and precipitations over the period JJAS 2000–2009. **(a)** 850 hpa geopotential heights (GPH) and monsoon circulation dust-induced anomalies calculated as the GPH difference between *dust* and *nodust* simulations. **(b)** Dust-induced precipitation anomaly. The dotted region defines statistically significant results at the 95 % confidence level. All modeling results represent a three-ensemble-member mean.

In order to further illustrate this point, we perform an additional experiment where the Indo-Pakistani dust sources are removed (*dust_noIP*). By analyzing the difference between *dust_noIP* and *dust* we see that taking into account the Indo-Pakistani sources results in an inhibition of convergence and precipitation over India (Fig. 12). Due to its geographic position and regional surface characteristics, the Indo-Pakistani dust source contributes relatively more than Arabia to the negative TOA radiative forcing and the dimming signal obtained over India. In this regard the Indo-Pakistani source-related effects tends to "compete" with the positive feedback associated with large radiative warming efficiencies over the Arabian Peninsula.

That said, it must be noted that radiative forcings and impacts might strongly depend on dust chemical composition and absorption/scattering properties (Miller et al., 2014; Perlwitz et al., 2001; Solmon et al., 2008), which exhibit a large

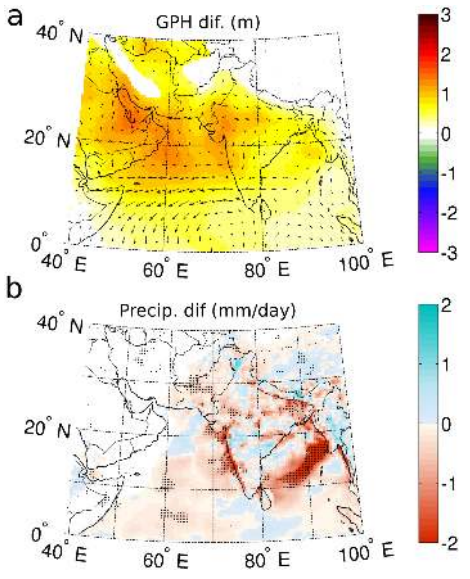

Figure 12. Impact of the Indo-Pakistani dust source compared to the dust simulation calculated as *dust_noIP* − *dust* over the period JJAS 2000–2009. **(a)** 850 hpa geopotential heights (GPH) and circulation change. **(b)** Precipitation changes. The dotted region defines statistically significant results at the 95 % confidence level. All modeling results represent a three-ensemble-member mean.

regional variability (Deepshikha et al., 2005) but are unfortunately poorly constrained by observations. In the present simulations we do not account for regional variation of dust refractive indices as proposed in recent studies (Scanza et al., 2015). This point might be especially important over the Indo-Pakistani region where simulated single-scattering albedo might be close to its critical value in relation to surface albedo: a slight change in optical properties and/or a misrepresentation of size distribution could result in a change in the sign of radiative forcing which can potentially result in an opposite dynamical feedback (in this case an enhancement of elevated heat pump effect over Pakistan and northern India). Some simple tests modifying dust single-scattering albedo values in RegCM4 and performed over the same domain tend to show that the more absorbing the dust, the more intense the positive feedback on convergence and precipitation over India is (S. Das, personal communication, 2015). Finally, note that we do not account for possible indirect dust effects on warm and ice cloud microphysics. There is still a considerable debate in this matter, and impacts are difficult to assess within the scope of the present study.

4.4 Coupling of Arabian dust increasing activity and precipitation variability over the 2000–2009 decade

Our working hypothesis is that, if the above mechanisms are valid, the observed increasing dust AOD trend over Arabia over the decade 2000–2010 might have been associated with, and perhaps contributing to, a positive impact on circulation and precipitation over southern India. Focusing on model results we see that, although the standard *dust* simulation is able to capture a slightly positive AOD trend over part of the Arabian Peninsula, this trend is nevertheless largely underestimated when compared to observations (Fig. 3a and b). Consistent with the arguments developed before, a likely reason for this underestimation is related to the fact that the cyclonic pattern found in reanalysis pentad differences is also not properly captured by the model as shown in Fig. 4b and c, meaning that the model does not properly reproduce increasing occurrences or/and intensification of Shamal conditions during the decade. These deficiencies are likely to be due to uncertainties in coupled convective and dynamical processes over the northern Arabian Sea, Pakistan and Bengal Gulf, which are extremely challenging to capture properly in climate models (Turner and Annamalai, 2012). In terms of dust AOD, the uncertainties in dust emissions parameterizations could further worsen errors in adequately simulating regional climatic trends (Evan et al., 2014).

However, since dust triggers a potentially important climatic feedback over the region, it is possible that failure to capture the increasing Arabian dust trend also contributes to failure to capture a proper trend in regional climate. To explore this issue, we perform an additional experiment in which dust emissions are forced in order to reproduce more realistically the observed JJAS AOD increasing trend (see Sect. 2.2 and Figs. 1a, 3b and c). This constraint is applied only over the Arabian Peninsula and eventual trends visible over other regions are primarily a result of Arabian dust transport or simulated spontaneously in response to simulated climate. In the JJAS AOD time series (Fig. 1a) we can note that the adjusted model shows enhanced AOD for DUSTY pentad relative to NONDUSTY pentad in a relatively similar way to observations. In terms of climatic impact, simulated circulation and surface pressure changes between NONDUSTY and DUSTY pentads show a rather different behavior depending on whether *nodust*, *dust* only or adjusted *dust_ft* simulations are considered (cf. Sect. 2), especially over the Arabian Sea and southern India (Fig. 4). With no dust, or when increasing dust emission tendency is not forced, the model tends to reproduce an anti-cyclonic pattern over the Arabian Sea (Fig. 4b and c) and no enhanced westward circulation toward the Indian coast, unlike what is observed in reanalyses (Fig. 4a). When dust tendency is forced, however, a westward convergence is obtained between 5 and 20° N, and surface pressure pentad differences over the Arabian Sea switch from positive to slightly negative (Fig. 8d). The cyclonic pattern and southward flow clearly seen in reanalyses is, however, not well reproduced by the simulation; it instead tends to generate a cyclonic pattern shifted to eastern India and Bengal Gulf. This indicates that dust radiative trends alone shall not be considered as the main driver for explaining regional circulation changes and also points out model limitations. With this in mind, the simulations still tend to show some relatively improved cir-

culation and surface pressure changes when dust is present and especially when the increasing dust trend is more realistically forced. From these results we suggest that while the cyclonic changes observed between pentad in reanalyses might be primarily a feature of climate variability, the likely associated increase in JJAS west-Asian dust emissions and Arabian Sea AODs could, however, determine a possibly important positive feedback contributing to the intensification of easterly circulation and humidity flux convergence towards the southwestern Indian coast. The simulated impact of this feedback on summer precipitation trends over southern India is depicted in Fig. 1b: simulated JJAS precipitations show an increasing linear trend in *dust_ft* deseasonalized JJAS simulations of about 0.11 mm day^{-1} year^{-1} and close to the value of the JJAS trend calculated from observations (0.13 mm day^{-1} year^{-1}), when no statistically significant trends are detected in *nodust* and *dust* simulations.

5 Conclusion

Overall our results emphasize the possible two-way interaction between dust emissions variability and the summer regional climate variability in the Indian monsoon domain for interannual to decadal timescales. Using observations and a regional climate model, we suggest that an increasing Arabian dust emission trends could have impacted the Indian monsoon circulation and contributed to the observed increasing 2000–2009 summer precipitation over southern India. There are potentially many global and regional players contributing to monsoon precipitation interannual and decadal variability (e.g., Indian Ocean Dipole, ENSO; Patra et al., 2005) and dust radiative forcing should not be considered as the main driver of the observed precipitation interannual and decadal variability. Dust radiative forcing might, however, determine a positive dynamical feedback favoring the establishment of lower-pressure conditions over the Arabian Sea likely associated with both enhanced Arabian dust emissions and precipitation over southern India. Please note, however, that the entire feedback loop has not been fully demonstrated here since we used forced emission trends.

This study does not consider any trend in anthropogenic aerosol emissions during the decade. Increasing AOD trends attributed to anthropogenic pollution have been measured over continental India, though they are mostly significant during the winter season (Babu et al., 2013). Nevertheless, it is likely there has been an impact of the anthropogenic aerosol trend on Monsoon rainfall during the studied decade, as for example discussed in Bollasina et al. (2011) (who conclude a general drying effect of anthropogenic aerosol in continental India). Note that in magnitude, the measured dust decadal AOD trends over Arabia and the Arabian Sea are equally if not more important than AOD trends attributed to pollution increase over India (Babu et al., 2013).

In view of these results, capturing the positive feedback between dynamics and dust emission trends in climate models could lead to a more realistic representation of decadal precipitation variability over India. This is even more relevant when considering the emergence and potential importance of "anthropogenic dust sources" as discussed in Ginoux et al. (2012). However, the present study, as well as Evan et al. (2014), shows that current dust parameterizations and implementations in climate and Earth system models have difficulties reproducing observed regional AOD interannual and decadal variability. Improvement of models – whether they deal with dust emissions processes, regional land use change or surface wind speed downscaling – is still of primary importance.

The Supplement related to this article is available online at doi:10.5194/acp-15-8051-2015-supplement.

Acknowledgements. The authors would like to thank two anonymous reviewers for their very useful comments, Jost von Hardenberg for providing aerosol large-scale fields for boundary conditions, R. Farneti and F. Kucharski for advices on slab-ocean implementation and scientific discussion as well as G. Giuliani and the RegCM developing team for maintaining and managing the code. The authors would also like to thank all the research teams involved in the creation and maintenance of the aerosol and precipitation observational products used in this study.

Edited by: Y. Balkanski

References

Ashouri, H., Hsu, K.-L., Sorooshian, S., Braithwaite, D. K., Knapp, K. R., Cecil, L. D., and Prat, O. P.: PERSIANN-CDR: Daily Precipitation Climate Data Record from Multi-Satellite Observations for Hydrological and Climate Studies, B. Am. Meteorol. Soc., 96, 69–83, doi:10.1175/BAMS-D-13-00068.1, 2015.

Babu, S. S., Manoj, M., Moorthy, K. K., Gogoi, M. M., Nair, V. S., Kompalli, S. K., Satheesh, S. K., Niranjan, K., Ramagopal, K., Bhuyan, P. K., and Singh, D.: Trends in aerosol optical depth over Indian region: Potential causes and impact indicators, J. Geophys. Res., 118, 11794–11806, 2013.

Balkanski, Y., Schulz, M., Claquin, T., and Guibert, S.: Reevaluation of Mineral aerosol radiative forcings suggests a better agreement with satellite and AERONET data, Atmos. Chem. Phys., 7, 81–95, doi:10.5194/acp-7-81-2007, 2007.

Bollasina, M. A., Ming, Y., and Ramaswamy, V.: Anthropogenic aerosols and the weakening of the South Asian summer monsoon, Science, 334, 502–505, 2011.

Bollasina, M. A., Ming, Y., and Ramaswamy, V.: Earlier onset of the Indian monsoon in the late twentieth century: The role of anthropogenic aerosols, Geophys. Res. Lett., 40, 3715–3720, 2013.

Brockwell, P. J. and Davis, R. A.: Introduction to time series and forecasting, Vol. 1, Taylor and Francis, 2002.

Cowan, T. and Cai, W.: The impact of Asian and non–Asian anthropogenic aerosols on 20th century Asian summer monsoon, Geophys. Res. Lett., 38, L11703, doi:10.1029/2011GL047268, 2011.

Das, S., Dey, S., and Dash, S.: Impacts of aerosols on dynamics of Indian summer monsoon using a regional climate model, Clim. Dynam., 44, 1685–1697, 2014.

Deepshikha, S., Satheesh, S., and Srinivasan, J.: Regional distribution of absorbing efficiency of dust aerosols over India and adjacent continents inferred using satellite remote sensing, Geophys. Res. Lett., 32, L03811, doi:10.1029/2004GL022091, 2005.

Dubovik, O. and King, M. D.: A flexible inversion algorithm for retrieval of aerosol optical properties from Sun and sky radiance measurements, J. Geophys. Res., 105, 20673–20696, 2000.

Emanuel, K. A.: A scheme for representing cumulus convection in large-scale models, J. Atmos. Sci., 48, 2313–2329, 1991.

Evan, A. T., Flamant, C., Fiedler, S., and Doherty, O.: An analysis of aeolian dust in climate models, Geophys. Res. Lett., 41, 5996–6001, 2014.

Ganguly, D., Rasch, P. J., Wang, H., and Yoon, J.-H.: Climate response of the South Asian monsoon system to anthropogenic aerosols, J. Geophys. Res., 117, D13209, doi:10.1029/2012JD017508, 2012.

Ginoux, P., Prospero, J. M., Gill, T. E., Hsu, N. C., and Zhao, M.: Global-scale attribution of anthropogenic and natural dust sources and their emission rates based on MODIS Deep Blue aerosol products, Rev. Geophys., 50, RG3005, doi:10.1029/2012RG000388, 2012.

Giorgi, F., Bi, X., and Qian, Y.: Indirect vs. direct effects of anthropogenic sulfate on the climate of East Asia as simulated with a regional coupled climate-chemistry/aerosol model, Climatic Change, 58, 345–376, 2003.

Giorgi, F., Coppola, E., Solmon, F., Mariotti, L., Sylla, M., Bi, X., and others: RegCM4: model description and preliminary tests over multiple CORDEX domains, Clim. Res., 52, 7–29, 2012.

Hamidi, M., Kavianpour, M. R., and Shao, Y.: Synoptic analysis of dust storms in the Middle East, Asia-Pac. J. Atmos. Sci., 49, 279–286, 2013.

Harris, I., Jones, P., Osborn, T., and Lister, D.: Updated high-resolution grids of monthly climatic observations – the CRU TS3. 10 Dataset, Int. J. Climatol., 34, 623–642, 2014.

Hsu, N. C., Gautam, R., Sayer, A. M., Bettenhausen, C., Li, C., Jeong, M. J., Tsay, S.-C., and Holben, B. N.: Global and regional trends of aerosol optical depth over land and ocean using SeaWiFS measurements from 1997 to 2010, Atmos. Chem. Phys., 12, 8037–8053, doi:10.5194/acp-12-8037-2012, 2012.

Huffman, G. J., Adler, R. F., Rudolf, B., Schneider, U., and Keehn, P. R.: Global precipitation estimates based on a technique for combining satellite-based estimates, rain gauge analysis, and NWP model precipitation information, J. Climate, 8, 1284–1295, 1995.

Jin, Q., Wei, J., and Yang, Z.-L.: Positive response of Indian summer rainfall to Middle East dust, Geophys. Res. Lett., 41, 4068–4074, 2014.

Kaufman, Y. J., Tanré, D., Dubovik, D. O., Karnieli, A., and Remer, L. A.: Absorption of sunlight by dust as inferred from satellite and ground-based remote sensing, Geophys. Res. Lett., 28, 1479–1482, 2001.

Kaskaoutis, D., Rashki, A., Houssos, E., Goto, D., and Nastos, P.: Extremely high aerosol loading over Arabian Sea during June 2008: The specific role of the atmospheric dynamics and Sistan dust storms, Atmos. Environ., 94, 374–384, 2014.

Kok, J. F.: A scaling theory for the size distribution of emitted dust aerosols suggests climate models underestimate the size of the global dust cycle, P. Natl. Acad. Sci. USA, 108, 1016–1021, 2011.

Kuhlmann, J. and Quaas, J.: How can aerosols affect the Asian summer monsoon? Assessment during three consecutive premonsoon seasons from CALIPSO satellite data, Atmos. Chem. Phys., 10, 4673–4688, doi:10.5194/acp-10-4673-2010, 2010.

Lamarque, J.-F., Bond, T. C., Eyring, V., Granier, C., Heil, A., Klimont, Z., Lee, D., Liousse, C., Mieville, A., Owen, B., Schultz, M. G., Shindell, D., Smith, S. J., Stehfest, E., Van Aardenne, J., Cooper, O. R., Kainuma, M., Mahowald, N., McConnell, J. R., Naik, V., Riahi, K., and van Vuuren, D. P.: Historical (1850–2000) gridded anthropogenic and biomass burning emissions of reactive gases and aerosols: methodology and application, Atmos. Chem. Phys., 10, 7017–7039, doi:10.5194/acp-10-7017-2010, 2010.

Lau, K., Kim, M., and Kim, K.: Asian summer monsoon anomalies induced by aerosol direct forcing: the role of the Tibetan Plateau, Clim. Dynam., 26, 855–864, 2006.

Lau, K.-M., Tsay, S. C., Hsu, C., Chin, M., Ramanathan, V., Wu, G.-X., Li, Z., Sikka, R., Holben, B., Lu, D., Chen, H., Tartari, G., Koudelova, P., Ma, Y., Huang, J., Taniguchi, K., and Zhang, R.: The Joint Aerosol–Monsoon Experiment: A new challenge for monsoon climate research, B. Am. Meteorol. Soc., 89, 369–383, 2008.

Mahowald, N. M.: Anthropocene changes in desert area: Sensitivity to climate model predictions, Geophys. Res. Lett., 34, L18817, doi:10.1029/2007GL030472, 2007.

Mahowald, N. M., Albani, S., Kok, J. F., Engelstaeder, S., Scanza, R., Ward, D. S., and Flanner, M. G.: The size distribution of desert dust aerosols and its impact on the Earth system, Aeolian Res., 15, 53–71, doi:10.1016/j.aeolia.2013.09.002, 2014.

Marbaix, P., Gallee, H., Brasseu, O., and van Ypersele, J.-P.: Lateral Boundary Conditions in Regional Climate Models: A Detailed Study of the Relaxation Procedure, Mon. Weather Rev., 131, 461–479, 2003.

Marticorena, B. and Bergametti, G.: Modeling the atmospheric dust cycle: 1. Design of a soil-derived dust emission scheme, J. Geophys. Res., 100, 16415–16430, 1995.

Martonchik, J. V., Diner, D. J., Kahn, R., Gaitley, B., and Holben, B. N.: Comparison of MISR and AERONET aerosol optical depths over desert sites, Geophys. Res. Lett., 31, L16102, doi:10.1029/2004GL019807, 2004.

Matsuura, K. and Willmott, C. J.: Terrestrial precipitation: 1900–2008 gridded monthly time series, Department of Geography Center for Climatic Research, University of Delaware, 2009.

Meehl, G. A., Arblaster, J. M., and Collins, W. D.: Effects of black carbon aerosols on the Indian monsoon, J. Climate, 21, 2869–2882, 2008.

Menut, L., Perez, C., Haustein, K., Bessagnet, B., Prigent, C., and Alfaro, S.: Impact of surface roughness and soil texture on min-

eral dust emission fluxes modeling, J. Geophys. Res., 118, 6505–6520, 2013.

Miller, R. L., Perlwitz, J. P., and Tegen, I.: Modeling Arabian dust mobilization during the Asian summer monsoon: The effect of prescribed versus calculated SST, Geophys. Res. Lett., 30, L22214, doi:10.1029/2004GL020669, 2004.

Miller, R. L., Knippertz, P., Pérez García-Pando, C., Perlwitz, J. P., and Tegen, I.: Impact of dust radiative forcing upon climate. In Mineral Dust: A Key Player in the Earth System. P. Knippertz, and J.-B.W. Stuut, Eds. Springer, 2014, 327–357, doi:10.1007/978-94-017-8978-3_13, 2014.

Moorthy, K. K., Nair, V. S., Babu, S. S., and Satheesh, S.: Spatial and vertical heterogeneities in aerosol properties over oceanic regions around India: Implications for radiative forcing, Q. J. Roy. Meteor. Soc., 135, 2131–2145, 2009.

Moulin, C., Gordon, H. R., Banzon, V. F., and Evans, R. H.: Assessment of Saharan dust absorption in the visible from Sea-WiFS imagery, J. Geophys. Res., 106, 18239–18250, doi:10.1029/2000JD900812, 2001.

Mulitza, S., Heslop, D., Pittauerova, D., Fischer, H. W., Meyer, I., Stuut, J. B., Zabel, M., Mollenhauer, G., Collins, J. A., and Kuhnert, H.: Increase in African dust flux at the onset of commercial agriculture in the Sahel region, Nature, 466, 226–228, 2010.

Nabat, P., Solmon, F., Mallet, M., Kok, J. F., and Somot, S.: Dust emission size distribution impact on aerosol budget and radiative forcing over the Mediterranean region: a regional climate model approach, Atmos. Chem. Phys., 12, 10545–10567, doi:10.5194/acp-12-10545-2012, 2012.

Nair, V. S., Babu, S. S., and Moorthy, K. K.: Aerosol characteristics in the marine atmospheric boundary layer over the Bay of Bengal and Arabian Sea during ICARB: Spatial distribution and latitudinal and longitudinal gradients, J. Geophys. Res., 113, D15208, doi:10.1029/2008JD009823, 2008.

Nair, V. S., Solmon, F., Giorgi, F., Mariotti, L., Babu, S. S., and Moorthy, K. K.: Simulation of South Asian aerosols for regional climate studies, J. Geophys. Res., 117, D04209, doi:10.1029/2011JD016711, 2012.

Nigam, S. and Bollasina, M.: "Elevated heat pump" hypothesis for the aerosol monsoon hydroclimate link: "Grounded" in observations?, J. Geophys. Res., 115, D16201, doi:10.1029/2009JD013800, 2010.

Notaro, M., Alkolibi, F., Fadda, E., and Bakhrjy, F.: Trajectory analysis of Saudi Arabian dust storms, J. Geophys. Res., 118, 6028–6043, 2013.

O'Brien, T. A., Sloan, L. C., and Snyder, M. A.: Can ensembles of regional climate model simulations improve results from sensitivity studies?, Clim. Dynam., 37, 1111–1118, 2011.

O'Brien, T. A., Chuang, P. Y., Sloan, L. C., Faloona, I. C., and Rossiter, D. L.: Coupling a new turbulence parametrization to RegCM adds realistic stratocumulus clouds, Geosci. Model Dev., 5, 989–1008, doi:10.5194/gmd-5-989-2012, 2012.

Ohara, T., Akimoto, H., Kurokawa, J., Horii, N., Yamaji, K., Yan, X., and Hayasaka, T.: An Asian emission inventory of anthropogenic emission sources for the period 1980–2020, Atmos. Chem. Phys., 7, 4419–4444, doi:10.5194/acp-7-4419-2007, 2007.

Patra, P. K., Behera, S. K., Herman, J. R., Maksyutov, S., Akimoto, H., and Yamagata, Y.: The Indian summer monsoon rainfall: interplay of coupled dynamics, radiation and cloud microphysics, Atmos. Chem. Phys., 5, 2181–2188, doi:10.5194/acp-5-2181-2005, 2005.

Perlwitz, J. P., Tegen, I., and Miller, R. L.: Interactive soil dust aerosol model in the GISS GCM: 1. Sensitivity of the soil dust cycle to radiative properties of soil dust aerosols, J. Geophys. Res., 106, 18167–18192, doi:10.1029/2000JD900668, 2001.

Qian, Y., Giorgi, F., Huang, Y., Chameides, W., and Luo, C.: Regional simulation of anthropogenic sulfur over East Asia and its sensitivity to model parameters, Tellus B, 53, 171–191, 2001.

Ramanathan, V., Chung, C., Kim, D., Bettge, T., Buja, L., Kiehl, J., Washington, W. M., Fu, Q., Sikka, D. R., and Wild, M.: Atmospheric brown clouds: Impacts on South Asian climate and hydrological cycle, P. Natl. Acad. Sci. USA, 102, 5326–5333, 2005.

Ramaswamy, V.: Influence of Tropical Storms in the Northern Indian Ocean on Dust Entrainment and Long–Range Transport, in: Typhoon Impact and Crisis Management, 149–174, Springer, 2014.

Reynolds, R. W., Rayner, N. A., Smith, T. M., Stokes, D. C., and Wang, W.: An improved in situ and satellite SST analysis for climate, J. Climate, 15, 1609–1625, 2002.

Rodwell, M. J. and Jung, T.: Understanding the local and global impacts of model physics changes: An aerosol example, Q. J. Roy. Meteor. Soc., 134, 1479–1497, doi:10.1002/qj.298, 2008.

Sayer, A. M., Hsu, N. C., Bettenhausen, C., Ahmad, Z., Holben, B. N., Smirnov, A., and Zhang, J.: SeaWiFS Ocean Aerosol Retrieval (SOAR): Algorithm, validation, and comparison with other data sets, J. Geophys. Res., 117, D03206, doi:10.1029/2011JD016599, 2012a.

Sayer, A. M., Hsu, N. C., Bettenhausen, C., Jeong, M.-J., Holben, B. N., and Zhang, J.: Global and regional evaluation of overland spectral aerosol optical depth retrievals from SeaWiFS, Atmos. Meas. Tech., 5, 1761–1778, doi:10.5194/amt-5-1761-2012, 2012b.

Scanza, R. A., Mahowald, N., Ghan, S., Zender, C. S., Kok, J. F., Liu, X., Zhang, Y., and Albani, S.: Modeling dust as component minerals in the Community Atmosphere Model: development of framework and impact on radiative forcing, Atmos. Chem. Phys., 15, 537–561, doi:10.5194/acp-15-537-2015, 2015.

Shalaby, A., Rappenglueck, B., and Eltahir, E. A. B.: The climatology of dust aerosol over the arabian peninsula, Atmos. Chem. Phys. Discuss., 15, 1523–1571, doi:10.5194/acpd-15-1523-2015, 2015.

Solmon, F., Giorgi, F., and Liousse, C.: Aerosol modelling for regional climate studies: application to anthropogenic particles and evaluation over a European/African domain, Tellus B, 58, 51–72, 2006.

Solmon, F., Mallet, M., Elguindi, N., Giorgi, F., Zakey, A., and Konaré, A.: Dust aerosol impact on regional precipitation over western Africa, mechanisms and sensitivity to absorption properties, Geophys. Res. Lett., 35, L24705, doi:10.1029/2008GL035900, 2008.

Sperber, K. R., Annamalai, H., Kang, I.-S., Kitoh, A., Moise, A., Turner, A., and Zhou, T.: The Asian summer monsoon: an intercomparison of CMIP5 vs. CMIP3 simulations of the late 20th century, Clim. Dynam., 41, 2711–2744, 2013.

Streets, D. G., Bond, T. C., Carmichael, G. R., Fernandes, S. D., Fu, Q., He, D., and Yarber, K. F.: An inventory of gaseous and

primary aerosol emissions in Asia in the year 2000, J. Geophys. Res., 108, doi:10.1029/2002JD003093, 2003.

Tawfik, A. B. and Steiner, A. L.: The role of soil ice in land–atmosphere coupling over the United States: A soil moisture–precipitation winter feedback mechanism, J. Geophys. Res., 116, D02113, doi:10.1029/2010JD014333, 2011.

Turner, A. G. and Annamalai, H.: Climate change and the South Asian summer monsoon, Nature Climate Change, 2, 587–595, 2012.

Vinoj, V., Rasch, P. J., Wang, H., Yoon, J.-H., Ma, P.-L., Landu, K., and Singh, B.: Short-term modulation of Indian summer monsoon rainfall by West Asian dust, Nat. Geosci., 7, 308–313, 2014.

Wang, C., Kim, D., Ekman, A. M., Barth, M. C., and Rasch, P. J.: Impact of anthropogenic aerosols on Indian summer monsoon, Geophys. Res. Lett., 36, L21704, doi:10.1029/2009GL040114, 2009.

Xia, X.: Variability of aerosol optical depth and Angstrom wavelength exponent derived from AERONET observations in recent decades, Environ. Res. Lett., 6, 44011–44019, 2011.

Yatagai, A., Kamiguchi, K., Arakawa, O., Hamada, A., Yasutomi, N., and Kitoh, A.: APHRODITE: Constructing a long–term daily gridded precipitation dataset for Asia based on a dense network of rain gauges, B. Am. Meteorol. Soc., 93, 1401–1415, 2012.

Yoshioka, M., Mahowald, N., Conley, A., Collins, W., Fillmore, D., and Coleman, D.: Impact of desert dust radiative forcing on Sahel precipitation: relative importance of dust compared to sea surface temperature variations, vegetation changes and greenhouse gas warming, J. Climate, 20, 1445–1467, 2007.

Zakey, A. S., Solmon, F., and Giorgi, F.: Implementation and testing of a desert dust module in a regional climate model, Atmos. Chem. Phys., 6, 4687–4704, doi:10.5194/acp-6-4687-2006, 2006.

Zakey, A. S., Giorgi, F., and Bi, X.: Modeling of sea salt in a regional climate model: Fluxes and radiative forcing, J. Geophys. Res., 113, D14221, doi:10.1029/2007JD009209, 2008.

Zhao, C., Liu, X., Ruby Leung, L., and Hagos, S.: Radiative impact of mineral dust on monsoon precipitation variability over West Africa, Atmos. Chem. Phys., 11, 1879–1893, doi:10.5194/acp-11-1879-2011, 2011.